

Identifying the interference effect in different harmonic-emission channels from oriented asymmetric molecules

Bing Zhang,^{1,*} Yanjun Chen,^{2,3,†} Xiangqian Jiang,¹ and Xiudong Sun¹

¹*Department of Physics, Harbin Institute of Technology, Harbin 150001, China*

²*College of Physics and Information Technology, Shaanxi Normal University, Xi'an 710062, China*

³*Beijing Computational Science Research Center, Beijing 100084, China*

(Received 28 August 2013; published 27 November 2013)

We investigate the effect of intramolecular interference in the high-order harmonic generation (HHG) from oriented asymmetric diatomic molecules interacting strongly with a laser field numerically. We focus on the two-center–interference–induced minimum in the two HHG channels of odd and even harmonics. As the interference usually results in a well-defined minimum for symmetric molecules, the odd or even HHG spectra of asymmetric molecules do not show a pronounced minimum in our simulations. We show that the interplay of different recombination routes, arising from the asymmetry of the molecule, significantly influences the minimum. A scheme is proposed to identify the interference effect in the odd versus even HHG spectra for diverse molecular parameters.

DOI: [10.1103/PhysRevA.88.053428](https://doi.org/10.1103/PhysRevA.88.053428)

PACS number(s): 32.80.Rm, 42.65.Ky

I. INTRODUCTION

High-order harmonic generation (HHG) has long been an active research topic in intense laser-matter interaction for its potential applications in molecular orbital imaging [1] and attosecond physics [2]. The HHG process can be well understood by the semiclassical [3] and quantum [4] recollision models: (i) ionization of the active electron by tunneling, (ii) propagation of the electron in the laser field, and (iii) recombination of the electron into the bound state to emit a high-energy photon.

In the last few decades, considerable efforts have been devoted to investigating the HHG from symmetric molecules, such as O₂ [5], N₂ [6], and H₂⁺ [7]. Lein and co-workers found that the harmonic spectrum of H₂⁺ shows a striking minimum [7]. Usually, this minimum can be read from the spectrum readily as it is located in a remarkably suppressed region in the HHG plateau. The position of the minimum is related to the orientation of the molecule and this phenomenon is identified as arising from intramolecular two-center interference. Thereafter, this striking minimum has attracted great theoretical and experimental interest [8–16] and has shown its significance in the molecular orbital tomography procedure [1].

For asymmetric molecules, such as CO [17–21], HeH²⁺ [22–24], NF [25], and BF [26], the minimum in the HHG spectrum has been less studied in comparison with symmetric ones. Recently, it has been shown that the difference between the recombination phases in different atomic centers plays a nontrivial role in this minimum [27]. The Stark effect originating from the permanent dipole [28,29] of the asymmetric molecule significantly influences this minimum [30]. In addition, the minimum is also shown to be sensitive to the valence orbital structure of the asymmetric molecule [31]. In the above studies, the minimum is associated with the whole HHG spectrum of the asymmetric molecule, including

both odd and even harmonics. The emission of odd and even harmonics is one of the important characteristics of the HHG from asymmetric molecules, which results from the symmetry breaking. To understand the HHG mechanism of the asymmetric molecule sufficiently, the property of these two HHG channels of odd and even harmonics also needs to be studied. In a previous paper with two-dimensional (2D) numerical simulations [32], it was shown that the two HHG channels of odd and even harmonics are subject to different interference effects. Very recently, it was also shown that through decoding odd-even harmonics, one can image the orbital of the asymmetric molecule [33]. In this situation, a detailed study of the interference minimum in odd versus even HHG spectra, which is important in asymmetric orbital imaging and can be used to judge the signs of the relevant dipoles, is desired.

In this paper, we study the HHG from asymmetric model diatomic molecules by numerically solving the time-dependent Schrödinger equation (TDSE) with full three-dimensional (3D) simulations. We pay attention to the interference-induced structure in the HHG spectra. Our simulations show that the odd or even HHG spectrum of the asymmetric molecule does not show a striking minimum in some cases. Our analyses reveal that, generally, there are several different recombination routes that contribute to the emission of odd or even harmonics, with a route dominating in the emission. For a certain energy region, however, as the dominating route is significantly suppressed due to two-center interference, other routes that are less influenced by the interference then become important in the emission. The interplay of the contributions from the different recombination routes washes out the striking minimum that may exist in the odd or even HHG spectrum due to two-center interference. In addition, as the asymmetry of the molecule is relatively weak, the excited state can also play an important role in the minimum. Since the effect of two-center interference within asymmetric molecules can entangle with other effects in the HHG of odd and even harmonics, we propose a scheme to identify the interference effect in these two HHG channels indirectly via the intersection of odd and even

*zhangbing@hit.edu.cn

†chenyjhb@gmail.com

spectra at the same orientation angle for the strong asymmetry of the molecule, as well as that of odd or even spectra at different angles for the weak asymmetry.

The paper is organized as follows. We present our numerical methods and discuss our main results in Sec. II. In Sec. III, we introduce the scheme to identify the interference effect in the HHG from asymmetric molecules. Section IV is our conclusion.

II. NUMERICAL METHODS AND DISCUSSIONS

In this part, to explore the interference effect in the HHG from asymmetric molecules, we first perform 3D recollision simulations. These simulations allow us to identify the role of the ionization process in the HHG. Because performing 3D full-quantum analyses of HHG is very time-memory consuming, one-dimensional (1D) analyses are then performed to study the role of the recombination process in the HHG. Finally, based on the 1D and 3D results, the interference effect for asymmetric molecules is discussed in detail through the analyses of the HHG recombination routes.

A. 3D recollision simulations: Role of ionization

In the 3D simulations, we assume the molecular axis is located in the xoy plane and the laser field is linearly polarized along a direction parallel to the x axis. The Hamiltonian of the asymmetric diatomic molecule studied here is given by $H(t) = \mathbf{p}^2/2 + V(\mathbf{r}) + \mathbf{r} \cdot \mathbf{E}(t)$ ($\hbar = e = m_e = 1$). Here, $\mathbf{E}(t) = f(t)\hat{\mathbf{e}}_x E \sin \omega_0 t$ is the external electric field and $\hat{\mathbf{e}}_x$ is the unit vector along the x axis. $f(t)$ is the envelope function. $V(\mathbf{r})$ is the Coulomb potential of the asymmetric molecule. We use the soft-core potential that has the following form: $V(\mathbf{r}) = -Z_1/\sqrt{\xi + r_1^2} - Z_2/\sqrt{\xi + r_2^2}$. Here $r_1^2 = (x - R_1 \cos \theta)^2 + (y - R_1 \sin \theta)^2 + z^2$, $r_2^2 = (x + R_2 \cos \theta)^2 + (y + R_2 \sin \theta)^2 + z^2$. Z_1 and Z_2 are the effective charges, $R_1 = Z_2 R / (Z_1 + Z_2)$ and $R_2 = Z_1 R / (Z_1 + Z_2)$. $R = 2$ a.u. is the internuclear separation. $\xi = 0.5$ is the smoothing parameter, and θ denotes the angle between the molecular axis and the laser polarization. Note that if $Z_1 = Z_2$, the above Hamiltonian stands for a symmetric molecule. In our calculations, we use a ten-cycle laser pulse which is linearly ramped up for three optical cycles and then keeps a constant intensity for seven additional cycles, similar to that used in Ref. [34]. This pulse form allows one to minimize the complications related to a time-varying pulse and to focus on the mechanism of the HHG from the asymmetric molecule that is subject to a particular intensity. It is a reasonable approximation to the usual case of a long laser pulse. We work with a grid size of $480 \times 60 \times 60$ a.u. for the x , y , and z axes, respectively. The coherent part of the HHG spectrum is given by

$$F(\omega, \theta) = \int \langle \psi(t) | \hat{\mathbf{e}}_x \cdot \nabla V(\mathbf{r}) | \psi(t) \rangle e^{i\omega t} dt, \quad (1)$$

where $|\psi(t)\rangle$ is the time-dependent wave function of the Hamiltonian $H(t)$ and ω is the emitted photon frequency.

To explore the role of the asymmetry in the HHG of asymmetric molecules, in the following discussions, we focus on two typical cases of $Z_1/Z_2 = 2$ and $Z_1/Z_2 = 1.33$. The

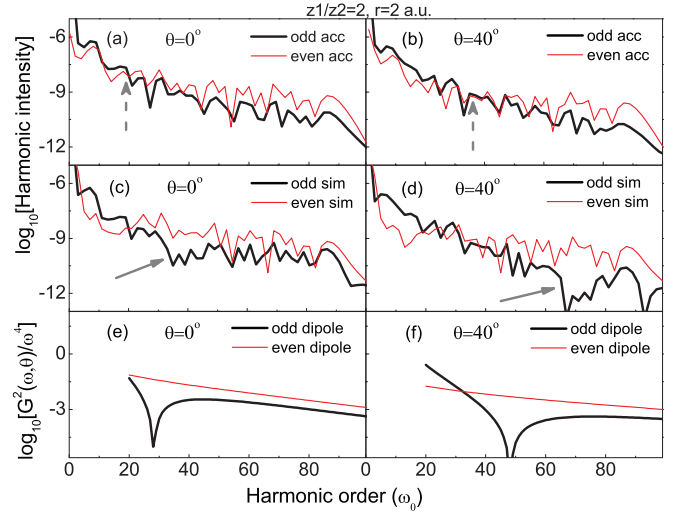


FIG. 1. (Color online) Harmonic spectra of a 3D asymmetric molecule exposed to a strong laser field with $I = 5 \times 10^{14}$ W/cm² and $\lambda = 800$ nm at (a),(c) $\theta = 0^\circ$ and (b),(d) $\theta = 40^\circ$. The odd (bold black curves) and even (thin red curves) harmonic spectra are obtained using (a),(b) Eq. (1) of the accurate expression and (c),(d) Eq. (2) of the simulated recollision. The molecular parameters are shown at the top of the panels. (e),(f) The corresponding odd $|G_{\text{odd}}(\omega, \theta)|^2/\omega^4$ of Eq. (7) (bold black curves) and even $|G_{\text{even}}(\omega, \theta)|^2/\omega^4$ of Eq. (8) (thin red curves) interference factors in dipoles. The dipole curves are divided by a factor ω^4 to compare with the spectra. Here, the dashed arrows indicate the intersection of the odd and even spectra and the solid arrows indicate the minimum in the odd-order simulated spectra.

former implies a larger asymmetry and the latter denotes a smaller one. In addition, to study the orientation dependence of the odd and even HHG spectra from asymmetric molecules, our discussions also concentrate on two typical cases of the small angle of $\theta = 0^\circ$ and the intermediate angle of $\theta = 40^\circ$. We mention that for the large angle of $\theta = 90^\circ$, the even harmonics disappear in the spectrum and the asymmetric molecule behaves similarly to an atom in our simulations. For comparison, the ground states of the asymmetric molecules with different molecular parameters studied here have the same ionization potential, $I_p = 1.1$ a.u. These ground states are chosen as the initial states in solving the TDSE numerically by means of the spectral method [35].

In the first rows of Figs. 1 and 2, we show the 3D HHG spectra obtained using Eq. (1) for asymmetric model diatomic molecules with different effective charges and orientation angles. In our simulations, odd and even harmonics are well resolved. In the paper, we will compare the odd and even spectra. For clarity, we use bold or thin lines to link them.

Due to the two-center characteristic of the asymmetric potential, one can expect that the effect of two-center interference will also induce a striking minimum in the odd-even HHG spectrum from the asymmetric molecule, as it does for the symmetric one H_2^+ [7]. However, from the results in Figs. 1(a) and 1(b) [and also in Figs. 2(a) and 2(b)], one does not observe any minimum that can be readily attributed to the geometrical two-center interference. What is the role of the asymmetric two-center potential in the HHG of odd and even harmonics? To answer this question, we first performed

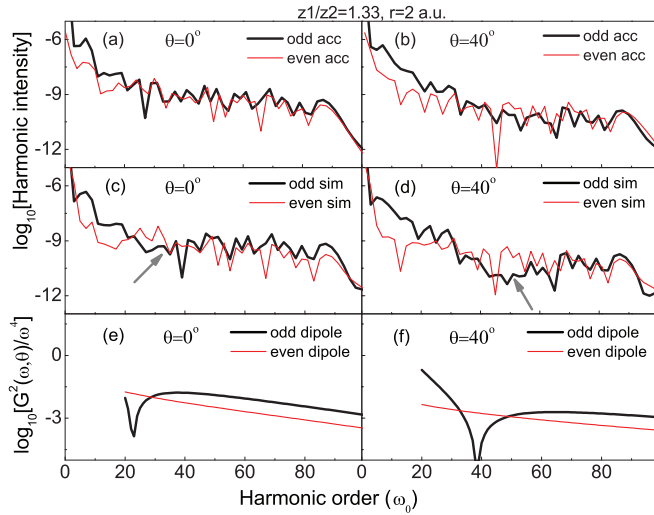


FIG. 2. (Color online) Same as Fig. 1, but for different molecular parameters.

a 3D recollision simulation. We use the continuum electronic wave packet generated from a symmetric molecule (H_2^+ used here) to recollide with the nuclei of the asymmetric one. The spectra generated from this recollision are given by

$$F_s(\omega, \theta) = \int \langle 0 | \vec{e}_x \cdot \nabla V(\mathbf{r}) | \psi_{sy}(t) \rangle a_0^*(t) e^{i\omega t} dt, \quad (2)$$

where $|\psi_{sy}(t)\rangle$ is the TDSE wave function of the symmetric molecule with the ionization potential as the asymmetric one, and $a_0(t) = \langle 0_{sy} | \psi_{sy}(t) \rangle$ and $|0_{sy}\rangle$ is the ground state of the symmetric molecule. $|0\rangle$ and $V(\mathbf{r})$ are associated with the asymmetric molecule under study.

It should be mentioned that in Eq. (2), (i) the continuum state components of the TDSE wave function $|\psi_{sy}(t)\rangle$ from the symmetric molecule can be assumed to be orthonormal to the ground state $|0\rangle$ of the asymmetric molecule. Because the continuum states are far away from the nuclei, the influence of the molecular potential on them is weak. One can expect that the continuum states of the asymmetric molecule are also similar to those of the symmetric one. (ii) The bound-state components of $|\psi_{sy}(t)\rangle$ cannot be considered to be orthonormal to the asymmetric ground state $|0\rangle$, since bound states are near to the nuclei and are affected strongly by the molecular potential, especially for lower bound states. This can influence the simulated spectra using Eq. (2). To check this influence, we have performed simulations with the exclusion of some lower-bound-state components of the symmetric molecule, obtained through the imaginary-time propagation, from the TDSE wave function $|\psi_{sy}(t)\rangle$. This procedure generates the spectra similar to those presented in Figs. 1 and 2, especially for the plateau harmonics. We, therefore, expect that the bound-state components of the symmetric molecule in $|\psi_{sy}(t)\rangle$ play a small role in the plateau harmonics obtained using Eq. (2). (iii) According to the three-step model [3,4], one can expect that the asymmetric potential will play roles in all of the ionization, propagation, and recombination processes of HHG. The use of Eq. (2) implies that here we only consider the role of the asymmetry in the recombination. For the closely related case of high-order above-threshold ionization, it has been shown [20]

that the asymmetry is also very important in the ionization process for some polar molecules. This is not accounted for by Eq. (2). However, as is shown in the following, for the present cases explored here, the asymmetry plays a small role in the ionization process and significantly influences the recombination.

The simulated spectra from Eq. (2) are shown in Figs. 1(c) and 1(d) [and also in Figs. 2(c) and 2(d)], in which both odd and even harmonics agree with the accurate TDSE results of Eq. (1) in most of the energy region. However, in the simulated odd-order harmonic spectra (the bold black curve), one can see a broad suppressed region with a striking minimum, as indicated by the solid arrows. This is similar to the case of the HHG from the symmetric molecule [7] and is expected to be associated with two-center interference. The agreement between the accurate and the simulated spectra indeed implies that the continuum-state electron wave packet generated from the asymmetric molecule is similar to the symmetric one in a wide energy region. For symmetric molecules, it has been shown [1] that the continuum-state electronic wave packets generated at different orientation angles are similar within a vertical scaling factor. The above agreement suggests that the conclusion also holds for the present asymmetric cases with small internuclear distances at which the permanent dipole movement is relatively weak. The reason is that in the tunneling region, the laser field is so strong that it causes an important distortion of the molecular potential. As a result, the molecular structure plays a small role in the ionization process through tunneling. This is one of the basic assumptions of the molecular orbital tomography procedure using HHG [1,33]. However, the disagreement between the accurate and the simulated spectra in the suppressed region also suggests that there exist some inherent differences. The differences show themselves remarkably in the energy region where the interference effect dominates. We will return to the 3D cases later.

B. 1D quantum analyses: Role of recombination

To understand this difference between the accurate and the simulated spectra in Figs. (1) and (2), next we perform simulations in 1D cases, where a full-quantum analysis of the HHG from asymmetric molecules can be executed. The 1D asymmetric Coulomb potential used here has the following form: $V(x) = -Z_1/\sqrt{0.5 + (x - R_1)^2} - Z_2/\sqrt{0.5 + (x + R_2)^2}$. We project $|\psi(t)\rangle$ on the eigenstates of the system and only consider the continuum-bound transition. Then we have $F(\omega, \theta) \approx \sum_n \int d\mathbf{p} [a_n(\mathbf{p}, \omega) \langle n | \vec{e}_x \cdot \nabla V | \mathbf{p} \rangle]$. Here, $a_n(\mathbf{p}, \omega) = \int dt [a_n^*(t) c_{\mathbf{p}}(t) e^{i\omega t}]$, $a_n(t) = \langle n | \psi(t) \rangle$, and $c_{\mathbf{p}}(t) = \langle \mathbf{p} | \psi(t) \rangle$. $\langle n | \nabla V | \mathbf{p} \rangle$ is the dipole moment between the continuum eigenstate $|\mathbf{p}\rangle$ and the bound eigenstate $|n\rangle$ of the field-free Hamiltonian $H_0 = \mathbf{p}^2/2 + V(x)$ of the 1D asymmetric molecule. Here, we only consider the contributions of the ground and the first excited states to the HHG, i.e., the cases of $n = 0$ and $n = 0, 1$. In our extended simulations, higher excited states contribute little to the HHG. Then we have

$$F_g(\omega, \theta) \approx \int d\mathbf{p} [a_0(\mathbf{p}, \omega) \langle 0 | \vec{e}_x \cdot \nabla V | \mathbf{p} \rangle] \quad (3)$$

for the ground-state channel and

$$F_{gf}(\omega, \theta) \approx \sum_{n=0,1} \int d\mathbf{p} [a_n(\mathbf{p}, \omega) \langle n | \vec{\mathbf{e}}_x \cdot \nabla V | \mathbf{p} \rangle] \quad (4)$$

for the ground–first-excited-states channel. Our simulations show that the ground state is mainly responsible for the HHG, while the excited state plays a smaller role here. For the ground-state channel given by Eq. (3), as discussed in Ref. [32], the main contribution to odd (even) harmonics comes from the continuum state $|\mathbf{p}\rangle$ with oddlike (evenlike) “parity.” Then we also have

$$F_g^{\text{odd}}(\omega, \theta) \approx \int d\mathbf{p} [a_0^{\text{u}}(\mathbf{p}, \omega) \langle 0 | \vec{\mathbf{e}}_x \cdot \nabla V | \mathbf{p}_u \rangle] \quad (5)$$

for the emission of odd harmonics and

$$F_g^{\text{even}}(\omega, \theta) \approx \int d\mathbf{p} [a_0^{\text{g}}(\mathbf{p}, \omega) \langle 0 | \vec{\mathbf{e}}_x \cdot \nabla V | \mathbf{p}_g \rangle] \quad (6)$$

for the emission of even harmonics. Here, $|\mathbf{p}_{u(g)}\rangle$ denotes the continuum state $|\mathbf{p}\rangle$ that has the ungeradelike (gerade-like) parity, $a_0^{\text{u(g)}}(\mathbf{p}, \omega) = \int dt [a_0^{\text{u(g)}}(t) c_{\mathbf{p}}^{\text{u(g)}}(t) e^{i\omega t}]$ and $c_{\mathbf{p}}^{\text{u(g)}}(t) = \langle \mathbf{p}_{u(g)} | \psi(t) \rangle$. We mention that while momentum eigenstates (plane waves) in the strong-field approximation [4] have exact parities, scattering states (continuum states) of asymmetric molecules have no parity. However, as discussed in Eq. (2), the influence of the molecular potential is weak on the continuum electrons, and scattering states of asymmetric molecules are similar to the symmetric ones, especially for the continuum electrons with high energy. We therefore use the terms of “geradelike” and “ungeradelike” to characterize the continuum states of asymmetric molecules. By comparison with Eq. (3), one can see that in Eq. (5), the contribution of the evenlike-parity continuum states to the emission of odd harmonics is omitted. The situation reverses for Eq. (6). Below, we will compare the HHG spectra obtained using the above expressions. One can expect that the comparison will provide insights into the complicated HHG mechanism of asymmetric molecules.

The relevant comparisons are shown in Figs. 3 and 4. In Fig. 3, we plot the results obtained for the 1D asymmetric molecule with the molecular parameters similar to those used in Fig. 1. The odd and even harmonic spectra obtained using Eq. (1) and their relevant dipoles $\langle 0 | \vec{\mathbf{e}}_x \cdot \nabla V | \mathbf{p}_u \rangle$ for odd harmonics and $\langle 0 | \vec{\mathbf{e}}_x \cdot \nabla V | \mathbf{p}_g \rangle$ for even harmonics are shown in the first row of Fig. 3. From Fig. 3(a), one can see that the yields of the even harmonics (thin red curve) are one order of magnitude higher than the odd harmonics (bold black curve) in the plateau. In addition, the interference-induced minimum is difficult to identify in the odd harmonics. These characteristics are similar to the 3D results in Fig. 1(a) and the corresponding 2D results in Ref. [32]. By comparison, the relative yields of odd versus even harmonics are well predicted by the relevant dipoles presented in Fig. 3(b) where the thin red curve of the even dipole, $\langle 0 | \vec{\mathbf{e}}_x \cdot \nabla V | \mathbf{p}_g \rangle$, is remarkably higher than the bold black curve of the odd one, $\langle 0 | \vec{\mathbf{e}}_x \cdot \nabla V | \mathbf{p}_u \rangle$. Another characteristic observed in Fig. 3(b) is that the bold black curve of the odd dipole shows a strikingly suppressed region with a sharp minimum. This characteristic can be expected to originate from the two-center characteristic of the molecular potential and is absent in the accurate odd spectrum in Fig. 3(a). However,

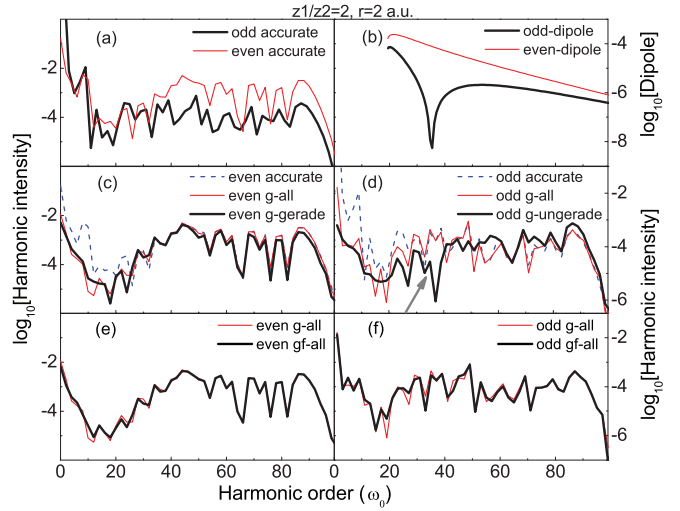


FIG. 3. (Color online) Harmonic spectra and relevant dipoles of a 1D asymmetric molecule exposed to a strong laser field with $I = 5 \times 10^{14}$ W/cm² and $\lambda = 800$ nm. The molecular parameters are shown at the top of the panels. (a) The accurate odd (bold black curves) and even (thin red curves) harmonic spectra obtained using Eq. (1). (b) The relevant dipoles $\langle 0 | \nabla V | \mathbf{p} \rangle^2 / \omega^4$ of the model molecule with $|\mathbf{p}\rangle$ being the oddlike parity $|\mathbf{p}_u\rangle$ (bold black curve) and evenlike parity $|\mathbf{p}_g\rangle$ (thin red curve) continuum eigenstates of the asymmetric molecule. The continuum energy E_p of $|\mathbf{p}\rangle$ is related to the harmonic ω using the disperse relation $E_p = \omega - I_p$. (c),(d) Comparison of the spectra obtained using Eq. (5) of the ground-state- $|\mathbf{p}_u\rangle$ channel, Eq. (6) of the ground-state- $|\mathbf{p}_g\rangle$ channel (bold black curves), Eq. (3) of the ground-state-all-continuum-states channel (thin red curves), and Eq. (1) of the accurate expression (dashed blue curves). (e),(f) Plot of the spectra obtained using Eq. (3) of the ground-state channel (thin red curves) and Eq. (4) of the ground–first-excited-states channel (bold black curves). Here, the solid arrows indicate the minimum in the spectra of Eq. (5).

when we calculate the spectrum using Eq. (4) where only the contribution from the continuum states with oddlike parity is considered, the characteristic is reproduced in our simulations.

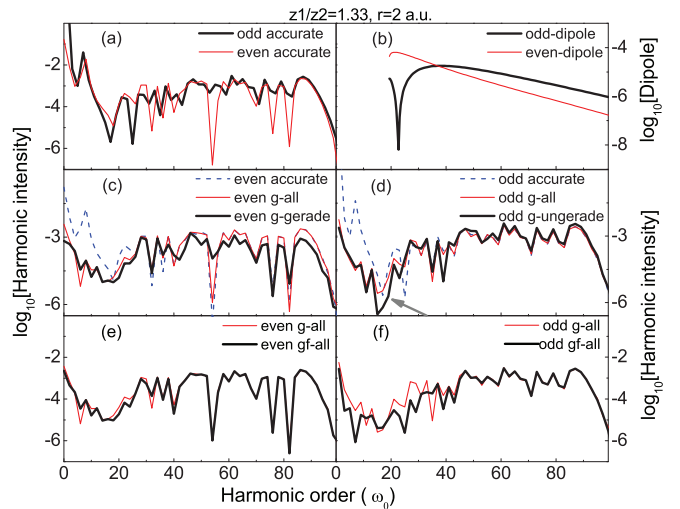


FIG. 4. (Color online) Same as Fig. 3, but for different molecular parameters.

In the second row of Fig. 3, we plot odd (even) HHG spectrum obtained from Eq. (5) [Eq. (6)] using bold black curves. Because the odd (even) spectrum is obtained with considering the transitions between the ground state and continuum states of oddlike (evenlike) parity, we call it odd g -ungerade (even g -gerade) spectrum. For comparison, the accurate spectrum obtained from Eq. (1) and that obtained from Eq. (3) with all continuum states are also plotted using dashed blue and thin red curves, respectively. It is obvious that the even harmonics obtained using different expressions in Fig. 3(c) are quite similar to each other in the plateau. This similarity indeed implies the applicability of Eq. (6) in describing the strong emission of even harmonics and the dominating recombination route from the ungeradelike-parity continuum state to the ground state in this emission.

As for odd harmonics in Fig. 3(d), the bold black curve presents a strikingly suppressed region around the 37th harmonic order, in agreement with the behavior of the odd-dipole curve in the upper panel, as indicated by the solid arrow. In this suppressed region, it differs from the other two curves significantly. In other regions, however, these three curves are also comparable. This difference between the spectra obtained using different expressions in Fig. 3(d) tells that in the region where the contribution from the oddlike-parity continuum states is suppressed significantly due to the interference effect, the evenlike-parity continuum states become important in the emission of odd harmonics. In other words, due to the strong suppression on the recombination route related to the oddlike-parity continuum state described by Eq. (5), another route from the evenlike-parity continuum state to the ground state dominates in the emission of the odd harmonics in a specific energy region.

It should be stressed that for a symmetric molecule with a gerade-parity initial state, the gerade-parity continuum states do not contribute to the emission of odd harmonics since the transition matrix element along the laser polarization \vec{e} is zero, i.e., $\langle 0_{\text{sy}}^{\text{gerade}} | \vec{e} \cdot \mathbf{r} | \mathbf{p}_{\text{sy}}^{\text{gerade}} \rangle = 0$. This is different from the asymmetric case discussed above.

C. HHG recombination routes for asymmetric molecules

More generally, for a system with the symmetric Coulomb potential, it is well known that the odd harmonics are emitted as the electron ionizes from and recombines with the same initial state that has a definite parity [4]. We denote the odd-harmonic route along the laser polarization \vec{e} simply using $\langle \mathbf{p} | \vec{e} \cdot \mathbf{r} | 0 \rangle_i \langle 0 | \vec{e} \cdot \mathbf{r} | \mathbf{p} \rangle_r$. The former matrix element $\langle \mathbf{p} | \vec{e} \cdot \mathbf{r} | 0 \rangle_i$ is related to the ionization process and the latter one $\langle 0 | \vec{e} \cdot \mathbf{r} | \mathbf{p} \rangle_r$ is related to the recombination process in the HHG. Note that for symmetric molecules, only as the initial state $|0\rangle$ and the continuum state $|\mathbf{p}\rangle$ have different parities, the values of the matrix elements are not zero.

For the asymmetric molecule with $1s\sigma$ initial state $|0\rangle = |0_g\rangle + |0_u\rangle$ that includes both gerade $|0_g\rangle$ and ungerade $|0_u\rangle$ components studied here, there are two HHG routes contributing to the emission of odd harmonics [33]. The first one corresponds to the gerade-parity component $|0_g\rangle$ of the initial state and can be denoted using $L_{gg}^o = \langle \mathbf{p}_u | \vec{e} \cdot \mathbf{r} | 0_g \rangle_i \langle 0_g | \vec{e} \cdot \mathbf{r} | \mathbf{p}_u \rangle_r$. This route is included in Eq. (5). The second one is related to the ungerade-parity component $|0_u\rangle$

of the initial state and can be denoted simply using $L_{uu}^o = \langle \mathbf{p}_g | \vec{e} \cdot \mathbf{r} | 0_u \rangle_i \langle 0_u | \vec{e} \cdot \mathbf{r} | \mathbf{p}_g \rangle_r$. This route is omitted in Eq. (5). When the first route L_{gg}^o dominates in the emission in most of the energy region, the second route L_{uu}^o shows itself in a specific energy region where the first one is significantly suppressed due to two-center interference. As a result, the interference-induced minimum arising from the first route is covered up by the contributions of the second route, as discussed in Fig. 3(d).

With the discussions, we return to 3D cases. In our 3D HHG recollision simulations, the continuum-state electron wave packet is generated from the symmetric molecule with the initial state having a gerade parity. Therefore, the second route L_{uu}^o discussed above, which is related to the tunneling ionization of the electron from the ungerade component, is closed. This implies that only the first route L_{gg}^o plays a role in the HHG recollision simulations. Consequently, we observe the striking interference minimum in the odd simulated spectra in the second rows of Figs. 1 and 2.

Similarly, the even harmonics are emitted as the electron ionizes from and returns to different components of the initial state. These relevant routes can be denoted simply using $L_{gu}^e = \langle \mathbf{p}_u | \vec{e} \cdot \mathbf{r} | 0_g \rangle_i \langle 0_u | \vec{e} \cdot \mathbf{r} | \mathbf{p}_g \rangle_r$ and $L_{ug}^e = \langle \mathbf{p}_g | \vec{e} \cdot \mathbf{r} | 0_u \rangle_i \langle 0_g | \vec{e} \cdot \mathbf{r} | \mathbf{p}_u \rangle_r$. In this case, the route L_{gu}^e , which is included in Eq. (6) and which is corresponding to the ionization of the electron from the gerade component of the initial state, still dominates in the emission. The dominating route is so strong that the other route, L_{ug}^e , which is omitted in Eq. (6) and is related to the ionization from the ungerade component of the initial state, does not show itself basically in the emission of even harmonics, as shown in Fig. 3(c). From the comparisons in Fig. 3(c), it is also safe to say that in comparison with the gerade component $|0_g\rangle$, there is only a small fraction of the ungerade component $|0_u\rangle$ of the asymmetric initial state to tunnel out from the asymmetric potential in the HHG process. As a result, the route L_{ug}^e has a small amplitude and thus contributes little to the emission of even harmonics.

In the last row of Fig. 3, we plot the odd and even harmonics obtained using Eq. (4) that considers the contributions of both the ground and the first excited states in bold black curves, which are very near to the thin red curves of the results of Eq. (3) where only the ground state is considered. This observation indicates that for the present case with the strong asymmetry, the main contribution to harmonics comes from the ground state.

In Fig. 4, we plot the HHG spectra and relevant dipoles of a 1D asymmetric molecule with molecular parameters similar to those used in Fig. 2. Despite the different parameter regions explored, we draw a similar conclusion from Fig. 4 as that from Fig. 3. The remaining difference between them is that in Fig. 4(a), with the relatively weak asymmetry, the yields of odd and even harmonics of the asymmetric molecule are close to each other, except for some oscillations in the even spectrum. In addition, the odd-harmonics route L_{uu}^o seems to play a smaller role in Fig. 4(d) than in Fig. 3(d), while the excited state shows a more important role in Fig. 4(f) than in Fig. 3(f).

We mention that (i) the minimum in Fig. 4(d) is below the ionization threshold. The interference model cannot work well in the energy region where the multiphoton effects are

expected to make an important contribution to harmonics. However, as seen in Fig. 4(b), the bold black curve of the odd dipole also shows a remarkable minimum, which is associated with two-center interference and is very near to the ionization threshold. Because of the close relation between dipoles and spectra discussed in Ref. [32], we expect that the interference effect also plays an important role in the minimum observed in Fig. 4(d). (ii) To check the important influence of the HHG recombination route L_{uu}^o on the interference minimum relating to the route L_{gg}^o , we have explored a wide parameter region in our extended simulations. (iii) The above discussions for the HHG recombination routes of asymmetric molecules also show that as the ionization process is not sensitive to the molecular structure, the recombination process mostly does so, similar to the symmetric cases [1]. (iv) As the HHG recombination routes are analyzed in detail in the 1D cases here, a 3D full-quantum analysis of HHG from asymmetric molecules, where the orientation effect can also be included, is highly desired.

Despite some limitations, from the above analyses, we arrive at the conclusion that for oriented asymmetric molecules, the disappearance of the striking interference minimum in odd or even spectra arises essentially from the inherent asymmetry of the molecule. This minimum is closely related to the structure of the asymmetric molecule [32,33]. The experimental procedures for orienting a polar molecule have also been reported recently [36,37], which is believed to have greatly stimulated relevant HHG experiments in the following years. Below, we will explore a scheme to “evaluate” this interference minimum in the odd-even HHG spectra.

III. SCHEMES TO IDENTIFY THE INTERFERENCE MINIMUM

In Ref. [32], the analytical expressions for the interference factors in the dipoles relating to the emission of odd and even harmonics have been given as follows:

$$G_{\text{odd}}(\omega, \theta) = a_1 \cos(p_k R_1 \cos \theta) + a_2 \cos(p_k R_2 \cos \theta) \quad (7)$$

for the emission of odd harmonics and

$$G_{\text{even}}(\omega, \theta) = a_1 \sin(p_k R_1 \cos \theta) - a_2 \sin(p_k R_2 \cos \theta) \quad (8)$$

for the emission of even harmonics. Here, it has been assumed that $a_1 = Z_1/B$, $a_2 = Z_2/B$, $B = \sqrt{Z_1^2 + Z_2^2}$, and $p_k = \sqrt{2\omega}$. In the last row of Fig. 1, we show the analytical results for odd and even interference factors using bold black and thin red curves. One can observe that the intersection of the relevant spectra in Fig. 1(a) is near to the 20th harmonic order, as indicated by the dashed arrow. This agrees with the intersection of the odd and even factors in Fig. 1(e). In Fig. 1(b), the intersection of the harmonic spectra is also located at an order similar to that predicted by the analytical model in Fig. 1(f). In particular, from Figs. 1(e) and 1(f), it can be seen that the minimum in the odd interference factor (bold black curve) is located at a position near to the intersection of the odd and even interference factors. Therefore, from the intersection of the odd and even harmonic spectra, one can predict the intersection of the relevant interference factors and roughly evaluate the position of the interference-induced minimum.

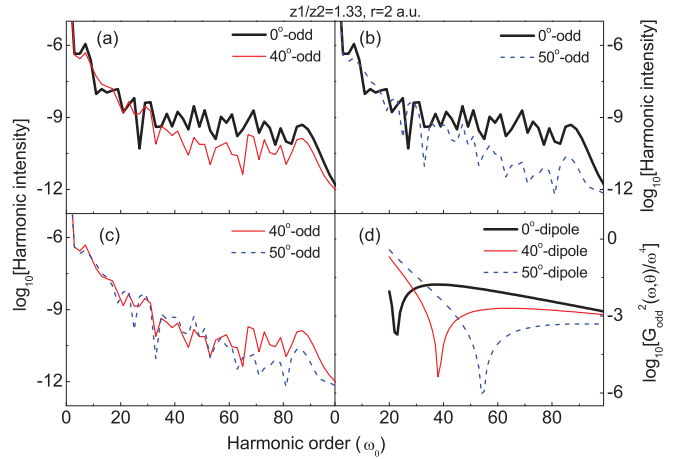


FIG. 5. (Color online) Odd-harmonic spectra obtained using Eq. (1) (a)–(c) and the corresponding interference factors $|G_{\text{odd}}(\omega, \theta)|^2/\omega^4$ of Eq. (7) (d) for a 3D asymmetric molecule exposed to a strong laser field with $I = 5 \times 10^{14}$ W/cm² and $\lambda = 800$ nm at $\theta = 0^\circ$ (bold black curves), $\theta = 40^\circ$ (thin red curves), and $\theta = 50^\circ$ (dashed blue curves). The molecular parameters are shown at the top of the panels.

The interference factors relating to the spectra in Figs. 2(a) and 2(b) are presented in the last row of Fig. 2. One can see that when the asymmetry of the molecule is relatively weak, the intersections of the spectra are not easy to identify because the yields of odd and even harmonics are comparable here. In this situation, how can one “evaluate” the interference-induced minimum in the spectra?

In Fig. 5, we plot the odd HHG spectra and the relevant interference factors of the asymmetric molecule with $Z_1/Z_2 = 1.33$ discussed in Fig. 2 at diverse orientation angles of $\theta = 0^\circ$, $\theta = 40^\circ$, and $\theta = 50^\circ$ using bold black, thin red, and dashed blue curves, respectively. For the model molecule with relatively weak asymmetry, the even HHG spectra at different angles are similar within a vertical scaling factor, but the odd spectra are sensitive to the angle. Therefore, the intersection of odd spectra at different angles can be clearly pointed out. Comparing the intersections of the odd spectra in Figs. 5(a)–5(c) with those of the related interference factors in Fig. 5(d), one can see that the intersection of spectra at $\theta = 0^\circ$ and $\theta = 40^\circ$ is located at about the 29th harmonic order, and so is that of the two relevant interference factors. Similarly, the intersection of spectra at $\theta = 0^\circ$ and $\theta = 50^\circ$ occurs at about the 34th order, and that of the two corresponding interference factors is around the 35th order. The position of the intersection in Fig. 5(c) also shows the agreement with that of the corresponding interference factors. Around the intersection, the curves of the interference factors at two different angles θ_1 and θ_2 go through their respective minima. These minima are also basically corresponding to the harmonics orders at which the relative yields of the harmonics at θ_1 and θ_2 have the maximal absolute values. Therefore, from the intersection phenomena for the odd spectra at two different angles, one can also approximately evaluate the interference minima in these spectra. Similar procedures have been proposed for symmetric molecules such as CO₂ [14] and discussed for the asymmetric molecule CO [33].

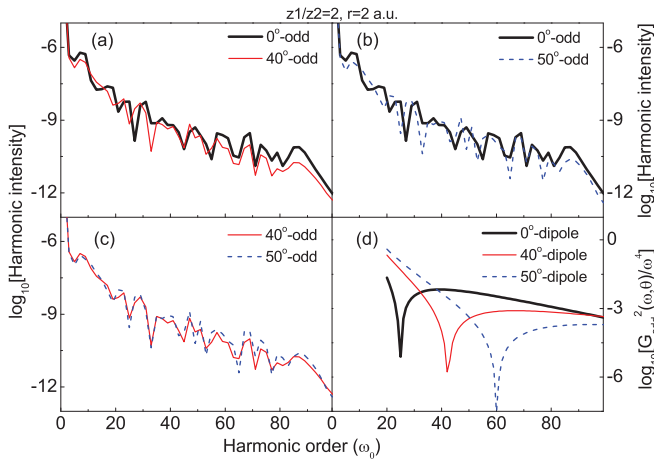


FIG. 6. (Color online) Same as Fig. 5, but for different molecular parameters.

In Fig. 6, we also compare the HHG spectra of the asymmetric molecule with the stronger asymmetry of $Z_1/Z_2 = 2$ at different orientation angles. Nevertheless, in this case, the odd-harmonic spectra seem not to be sensitive to the angle θ , and it is hard to tell the position of the intersection of the spectra at different angles. So the above procedure may not be suitable for an asymmetric molecule with strong asymmetry.

Now, we can summarize our schemes for evaluating the interference-induced minimum through the intersection of the HHG spectra of asymmetric molecules as two complementary procedures: one is predicting the minimum from the intersection of odd and even spectra at the same angle, which is suitable for the molecule of strong asymmetry, and the other is

forecasting the minimum from the intersection of odd or even spectra at different orientation angles, which can be used for the molecule of weak asymmetry.

IV. CONCLUSION

In summary, we have investigated the interference effect in the HHG from asymmetric molecules with varied parameters. Our 3D simulations show that the two HHG channels of odd and even harmonics are significantly affected by different interference effects, in agreement with the previous 2D predictions. Our further analyses show that each HHG channel of odd and even harmonics follows several different recombination routes arising from the intrinsic property of the asymmetric molecule. It is the interplay of the different routes in the HHG process that leads to the difficulty in identifying the interference-induced minimum in the odd or even HHG spectrum from the asymmetric molecule. In this situation, we propose a scheme to “evaluate” the interference minimum using the intersection of the odd versus even HHG spectra at the same or different orientation angles. The results give suggestions on imaging the structure of the asymmetric molecule using HHG.

ACKNOWLEDGMENTS

We thank the referees for their important suggestions in improving the paper. This work was supported by the National Basic Research Program of China (Grant No. 2013CB328702), NNSF Grants No. 11274090 and No. 11104225, CAEP Foundation Project No. 2011B0102031, and the Fundamental Research Funds for the Central Universities (Grant No. HIT.NSRIF.2011013).

- [1] J. Itatani, J. Levesque, D. Zeidler, Hiromichi Niikura, H. Pepin, J. C. Kieffer, P. B. Corkum, and D. M. Villeneuve, *Nature (London)* **432**, 867 (2004).
- [2] P. B. Corkum and F. Krausz, *Nat. Phys.* **3**, 381 (2007).
- [3] P. B. Corkum, *Phys. Rev. Lett.* **71**, 1994 (1993).
- [4] M. Lewenstein, Ph. Balcou, M. Yu. Ivanov, Anne L’Huillier, and P. B. Corkum, *Phys. Rev. A* **49**, 2117 (1994).
- [5] J. Itatani, D. Zeidler, J. Levesque, M. Spanner, D. M. Villeneuve, and P. B. Corkum, *Phys. Rev. Lett.* **94**, 123902 (2005).
- [6] Y. Mairesse, J. Higuier, N. Dudovich, D. Shafir, B. Fabre, E. Mével, E. Constant, S. Patchkovskii, Z. Walters, M. Yu. Ivanov, and O. Smirnova, *Phys. Rev. Lett.* **104**, 213601 (2010).
- [7] M. Lein, N. Hay, R. Velotta, J. P. Marangos, and P. L. Knight, *Phys. Rev. Lett.* **88**, 183903 (2002).
- [8] R. de Nalda, E. Heesel, M. Lein, N. Hay, R. Velotta, E. Springate, M. Castillejo, and J. P. Marangos, *Phys. Rev. A* **69**, 031804(R) (2004).
- [9] T. Kanai, S. Minemoto, and H. Sakai, *Nature (London)* **435**, 470 (2005).
- [10] C. Vozzi, F. Calegari, E. Benedetti, J. P. Caumes, G. Sansone, S. Stagira, M. Nisoli, R. Torres, E. Heesel, N. Kajumba, J. P. Marangos, C. Altucci, and R. Velotta, *Phys. Rev. Lett.* **95**, 153902 (2005).
- [11] Anh-Thu Le, X. M. Tong, and C. D. Lin, *Phys. Rev. A* **73**, 041402(R) (2006).
- [12] M. Lein, *J. Phys. B* **40**, R135 (2007).
- [13] S. Baker, J. S. Robinson, M. Lein, C. C. Chirila, R. Torres, H. C. Bandulet, D. Comtois, J. C. Kieffer, D. M. Villeneuve, J. W. G. Tisch, and J. P. Marangos, *Phys. Rev. Lett.* **101**, 053901 (2008).
- [14] Y. J. Chen, J. Liu, and Bambi Hu, *J. Chem. Phys.* **130**, 044311 (2009); Y. J. Chen and Bambi Hu, *ibid.* **131**, 244109 (2009).
- [15] S. Odžak and D. B. Milošević, *Phys. Rev. A* **79**, 023414 (2009).
- [16] O. Smirnova, Y. Mairesse, S. Patchkovskii, N. Dudovich, D. Villeneuve, P. Corkum, and M. Yu. Ivanov, *Nature (London)* **460**, 972 (2009).
- [17] J. Heslar, J. J. Carrera, D. A. Telnov, and S. I. Chu, *Int. J. Quantum Chem.* **107**, 3159 (2007).
- [18] A. Etches and L. B. Madsen, *J. Phys. B* **43**, 155602 (2010).
- [19] B. B. Augstein and C. Figueira de Morisson Faria, *J. Mod. Opt.* **58**, 1173 (2011).
- [20] M. Busuladžić, E. Hasović, W. Becker, and D. B. Milošević, *J. Chem. Phys.* **137**, 134307 (2012).
- [21] S. Odžak and D. B. Milošević, *J. Opt. Soc. Am. B* **29**, 2147 (2012).
- [22] X. B. Bian and A. D. Bandrauk, *Phys. Rev. Lett.* **105**, 093903 (2010).

- [23] X. B. Bian and A. D. Bandrauk, *Phys. Rev. A* **86**, 053417 (2012).
- [24] X. Y. Miao and H. N. Du, *Phys. Rev. A* **87**, 053403 (2013).
- [25] B. B. Augstein and C. Figueira de Morisson Faria, *J. Phys. B* **44**, 055601 (2011).
- [26] J. Heslar, D. Telnov, and Shih-I. Chu, *Phys. Rev. A* **83**, 043414 (2011).
- [27] X. Zhu, Q. Zhang, W. Hong, P. Lan, and P. Lu, *Opt. Express* **19**, 436 (2011).
- [28] G. L. Kamta and A. D. Bandrauk, *Phys. Rev. Lett.* **94**, 203003 (2005).
- [29] E. Hasović, M. Busuladžić, W. Becker, and D. B. Milošević, *Phys. Rev. A* **84**, 063418 (2011).
- [30] A. Etches, M. B. Gaarde, and L. B. Madsen, *Phys. Rev. A* **84**, 023418 (2011).
- [31] A. Rupenyan, P. M. Kraus, J. Schneider, and H. J. Wörner, *Phys. Rev. A* **87**, 031401(R) (2013); **87**, 033409 (2013).
- [32] Y. J. Chen and B. Zhang, *Phys. Rev. A* **84**, 053402 (2011).
- [33] Y. J. Chen, L. B. Fu, and J. Liu, *Phys. Rev. Lett.* **111**, 073902 (2013).
- [34] J. L. Krause, K. J. Schafer, and K. C. Kulander, *Phys. Rev. A* **45**, 4998 (1992).
- [35] M. D. Feit, J. A. Fleck, Jr., and A. Steiger, *J. Comput. Phys.* **47**, 412 (1982).
- [36] S. De, I. Znakovskaya, D. Ray, F. Anis, Nora G. Johnson, I. A. Bocharova, M. Magrakvelidze, B. D. Esry, C. L. Cocke, I. V. Litvinyuk, and M. F. Kling, *Phys. Rev. Lett.* **103**, 153002 (2009).
- [37] E. Frumker, C. T. Hebeisen, N. Kajumba, J. B. Bertrand, H. J. Wörner, M. Spanner, D. M. Villeneuve, A. Naumov, and P. B. Corkum, *Phys. Rev. Lett.* **109**, 113901 (2012).